

Model Error Maps as robust features for T1/T2-weighted data segmentation

U. S. Rudrapatna¹, A. van der Toorn¹, I. A. Tiebosch¹, J. P. Pluim¹, and R. M. Dijkhuizen¹

¹University Medical Center Utrecht, Utrecht, Netherlands

Introduction: Segmentation of MR images into regions of differing relaxivities (R_1 and R_2) is usually performed with data intensities¹ and parametric maps² as primary features. At low SNR, the efficacy of these features decreases. In this study, we propose a strategy to derive robust primary features to overcome this difficulty and show that these can either replace or supplement the ones currently used.

Method: We assume that the time series at each pixel location of T₁- and T₂-weighted data can be modeled as f_1 and f_2 , respectively (eqns.1, 2, shown below). The proposed strategy is based on the observation that, the fewer the parameters we need to estimate from a time series, the smaller the variability³. R_1 and R_2 mapping involve estimation of both A and λ . Suppose we pretend that we know λ at a pixel location, we are left with a linear problem of estimating A , to approximate f . We hypothesize that the pixel-wise least-squares-fit error due to an assumed λ (λ_v) and an estimated A can discriminate regions with differing relaxivities better than the λ s estimated by R_1 and R_2 mapping. By varying λ_v over a set Λ_v created from a priori knowledge, we form a set of "Model error maps" (MEMs). By MaxRel⁴, mRMR⁴ and F-score⁵ feature selection studies, we show that families of such error maps can be more useful starting materials for supervised or unsupervised segmentation than intensities or parametric maps. In our study, two functions of least-squares error are used, Ψ_1 and Ψ_2 (eqns.4, 5), closely related to Ψ_0 (eqn.3), the log-likelihood function of hypothesis testing for the alternate hypothesis f_1 or f_2 with parameter λ_v . \hat{f} denotes f_i with estimated A , for a given λ_v . We analyze the proposed method under both Gaussian and Rician noise models (Gnm and Rnm, respectively). We use Maximum Likelihood (ML) estimators⁶ for R_1 and R_2 mapping and for estimating A to obtain MEMs. Under Gnm, the ML estimator of A is equivalent to the MVU³. MLEs under Rnm need knowledge of noise variance, which we assumed we knew (in practice, they can be estimated from noise-only samples). The MLEs were based on simplex minimization with 20 random starts.

Experiments: Using R_1 maps of brains of in-vivo adult male Wistar rats scanned at 4.7T (28 points (N) scanned with δ_{ti} of 0.15s), we obtained R_1 values typically found in white and gray matter, basal nuclei and arteries (denoted as Λ_{fl} in Fig.1). For every $\lambda \in \Lambda_{fl}$, we generated 10^3 time series (f_i) with same N and δ_{ti} at a specified SNR by adding Rician noise ($\sigma^2=0.1$, A depended on SNR). We associated class labels to each time series based on the underlying λ . Thus, we constructed a 5 class dataset with 10^3 realizations for each class. These data were used to estimate the R_1 values and MEMs from Ψ_1 and Ψ_2 by assuming Gnm first and Rnm next. Thus we had 94 measurements for each time series- 28 intensities+2 R_1 values (assuming Gnm and Rnm)+32 Ψ_1 values (16 each for Gnm and Rnm with $\lambda_v \in \Lambda_{v1}$)+32 Ψ_2 values (similar to Ψ_1). We then analyzed the ability of these measurements in being able to discriminate the 5 underlying classes by treating them as features, and ranking them according to 3 feature selection criteria. The study was repeated at 4 SNRs ($\langle A \rangle / \sigma = 5, 8, 12, 20$) and with data combined from all SNRs (to simulate coil sensitivity variation). Similar studies were performed on T₂-weighted data, but with model f_2 , N=12, $\delta_{te}=0.015s$ and $\lambda_v \in \Lambda_{v2}$. In this case, we were left with 78 features since we had only 12 intensities.

Results: Fig.1 shows top 50 ranks obtained by the features in both studies under various conditions. Darker regions denote better features (black= Rank 1). R_1 and R_2 denote parametric maps, and Ψ_i denote MEMs obtained with Ψ_i . Each strip of F-score/MaxRel/mRMR has 5 horizontal sub-strips. The first four correspond to increasing SNR, while the fifth is the result obtained from the combined study (denoted as c in mRMR strip). Thus, in both studies, each feature was ranked 15 times (5SNRx3 Ranking criteria). T₁-weighted data studies showed that 13 out of 15 times, an MEM features claimed the top rank. R_1 mapping under Gnm ranked the best twice, but under the relatively less reliable F-score, and only at high SNRs (12, 20). Choosing the right noise model made a difference in this study, especially at low SNR. In studies on T₂-weighted data, the R_2 maps performed poorly in comparison to MEMs (best rank was 17). The MEM features ranked the best again, except for one case, endorsing our hypothesis. At low SNR, results from both studies indicate that we benefit by combining intensities with MEMs. The two most important results from this study are (i) that all ranking methodologies rate MEMs far higher than scaled intensities and R_1 and R_2 maps in both the studies, under all SNRs, clearly corroborating our hypothesis (unscaled intensities gave poorer results) and (ii) that the choice of Λ_{vi} were not as critical as their range. Fig.2 shows results of k-means clustering (14 clusters) a T₁-weighted dataset with two different feature sets. The first used 16 MEMs (Ψ_1 on Λ_{v1}) and the second used intensities (N=28) in conjunction with R_1 map (all under Gnm). With nearly half the number of features, MEMs gave less noisy segmentation. Fig.3 shows similar results with 5 clusters from a T₂-weighted dataset (N=12) which had low SNR, with 3 feature sets. The first used 16 MEMs (Ψ_2 on Λ_{v2}), the second used intensities with R_2 map and the third result used only intensities. Clearly, we see that MEMs show less unwanted spatial variations compared to the second result, as expected, and recognize the lesion in the basal nuclei clearly. With intensities alone, the lesion could not be discerned. Though k-means is not a bench mark segmentation algorithm, we used it to confirm our hypothesis, that MEMs can be very effective primary features for segmentation. As an independent set of features, or as supplements to intensities and parametric maps, these offer promising applications, given the fact that there may be more to gain by choosing the right Λ_{vi} and more importantly, other Ψ s. The demonstration of this possibility is the main contribution of this work.

$$f_1(A, \lambda, n) = A * \text{abs}(1 - 2 * \exp(-\lambda t_i(n))) + w(n) - 1 \quad f_2(A, \lambda, n) = A * \exp(-\lambda t_e(n)) + w(n) - 2 \quad \Psi_0(y, \lambda) = -\left(\sum_i^N (y(n) - \hat{f}(\lambda, n))^2 - \sum_i^N y(n)^2\right) - 3$$

$$\Psi_1(y, \lambda_v) = \sum_i^N (y(n) - \hat{f}(\lambda_v, n))^2 / \sum_i^N y(n)^2 - 4 \quad \Psi_2(y, \lambda_v) = (\Psi_0(y, \lambda) - \min(\Psi_0(y, \lambda))) / (\max(\Psi_0(y, \lambda)) - \min(\Psi_0(y, \lambda))) - 5$$

References: [1] D.L.Pham et al., IEEE Trans.Med.Imaging,18(9):737-752,1999. [2] Robin de Graaf et al., PNAS, 34(101):12700-12705. [3] Fundamentals of Statistical Signal Processing: Estimation/Detection Theory - Steven Kay. [4] Peng et al., IEEE Trans. Pattern Analysis and Machine Intelligence, 27(8):1226-1238, 2005. [5] Feature Extraction: Foundations and Applications, Isabella Guyon et al., Springer, 2006. [6] J M Bonny et al., MRM, 36:287-293, 1996.

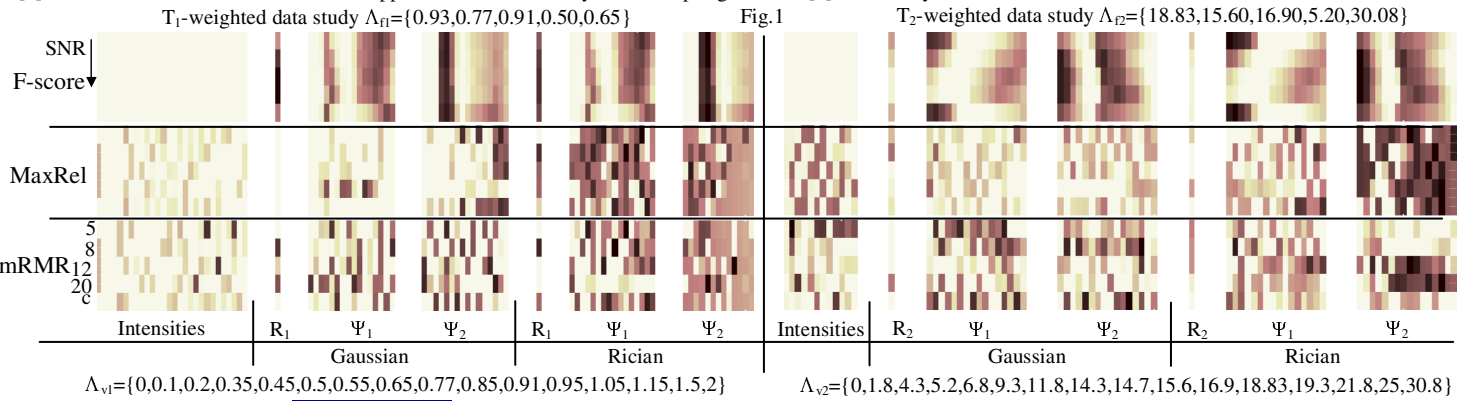


Fig.2 Clustering results for T₁-weighted data. left- MEMs, right-Intensities+ R_1 map

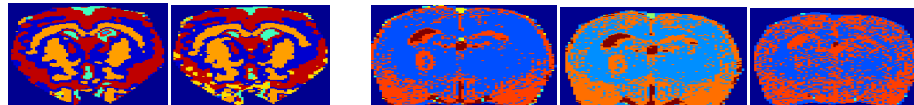


Fig. 3 Clustering results for T₂-weighted data. left-MEMs Center-Intensities+ R_2 map, right-Intensities